PUBLISHING HOUSE
OF THE ROMANIAN ACADEMY

PROCEEDINGS OF THE ROMANIAN ACADEMY, Series A,
Volume 3, Number 3/2002.

INTERFACE EFFECTS IN METAL-C_{60} THIN FILM NANOSYSTEMS

Rodica MANAILA*, Dan MACOVEI**, Sorin POENARIU**, Andrei DEVENYI*

* Center for Advanced Studies in Physics of the Romanian Academy
**National Institute for Physics of Materials, POB MG – 7, RO – 76900 Bucharest – Magurele,
Corresponding author: Andrei DEVENYI, E-mail:devenyi@alpha1.infim.ro

Thin-film nanosystems metal (M)–fullerite C_{60} are best suited for investigating interface interaction processes. A coordinated series of physical methods revealed the primordial importance of charge transfer from metal nano–clusters to C_{60}. On the other hand, formation of hybrid M-C orbitals can occur, depending on the structure of electronic levels of M, i.e. on its nature. Both effects cause considerable alterations in the structure and occupation of electronic levels of the C_{60} matrix and open a perspective for preparing thin films with controlled physical properties.

Key words: C_{60}, fullerite, nano – systems

1. INTRODUCTION

Metal–C_{60} interface interaction enjoys nowadays an increasing scientific and applicative interest. At the interface of a metal with fullerite (the fcc crystalline form of C_{60}), a wealth of phenomena were recently reported, with two main aspects [1]:

- charge transfer metal $\rightarrow$ C_{60}, until egalization of Fermi levels.

- formation of hybrid orbitals (e.g. metal s, d–C_{60} π, π^*), depending on the distribution of electronic levels in both solids.

The metal–C_{60} interface is usually investigated in bi–layers (e.g. a C_{60} monolayer (ML) or thicker layers deposited on a single–crystal metal surface). Charge transfer was mainly documented using Raman spectroscopy [2, 3], where the C_{60} $A_g(2)$ mode shows a "red shift", proportional to the negative charge received. UV-VIS photoemission spectroscopy revealed the structure of valence band (HOMO) in C_{60} ML's deposited on well–defined metal surfaces. HOMO bands shifts and broadening were reported [1, 4, 5], due to orbital hybridization, as well as a new occupied band (below E_F), originating in LUMO states, filled by charge transfer. The latter effect causes the C_{60} layer to become conducting [6]. Hybridization also affects LUMO empty states at the interface, as shown by inverse photoemission [7], X-ray absorption [4, 6] and carbon deep level photoemission [1].

2. PREPARATION OF METAL-C_{60} NANOSTRUCTURES

The present work was intended to look for interface interaction in metal–C_{60} nanostructures, much better suited to this purpose than bi–layers, due to the high specific interface area (despite a lack of crystallographic definition of metal surface). In clusters 3–5 nm in size, surface atoms can reach 50 % of the total atom number. Also, a comparison will be made between two systems: Cu/C_{60} (where charge transfer prevails) and Ni/C_{60} (where orbital hybridization is dominant). Characteristic effects of these two types of interaction on various properties of the C_{60} matrix will be discussed.

Metal (M)–C_{60} nanostructures were prepared [8 - 11] as co–evaporated thin films, comprising M (Cu, Ni) nanoclusters embedded in a fullerite matrix. The metal concentration range was 0.6 – 35.7 at% (Cu) and 10.4 – 20.7 at% (Ni).

Due to the extended interface area, new evidence was found on the different interaction aspects, depending on the metal nature. Several methods were used: Raman, X–ray absorption (EXAFS) and emission (XES) spectroscopies, X–

ray diffraction (XRD), electron microscopy (EM), as well as electrical transport to gather new evidence on interface phenomena.

3. RESULTS
3.1 RAMAN SPECTROSCOPY OF C_{60} INTRAMOLECULAR VIBRATIONS

Mode $A_g(2)$ ("pentagon pinch") of the C_{60} cage is particularly sensitive to the negative charging, due to the lowering of C – C bond force constant. In Cu – C_{60} thin films (35.8 at % Cu) a satellite can be noticed (Fig. 1), with a red shift of~ 20 ± 1 cm^{-1} [3]. Following a linear calibration [12], it suggests a negative charge of 3.3 ± 0.1 e^- / C_{60}, presumably in the fullerite zones surrounding Cu clusters. Also, moderate activation of "silent" and sum modes is noticed (e.g. increase of $H_g(8)$ in Fig. 1), attributed to slight symmetry distortions of the C_{60} cage due to interface interaction, including the effect of surface plasmons in Cu clusters. Still, the main Ag(2) band remains relatively narrow.

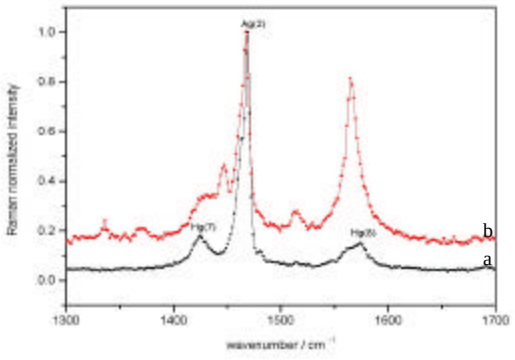

Fig.1 Raman spectra of a: C_{60} and b: $Cu_{33.4}C_{60}$ films (λ_{exc} = 514.5 nm). Intensity data are normalized to the highest values.

In Ni/C_{60} films, the Ag(2) band becomes very broad (Fig. 2), suggesting strong distortions of the C_{60} cage, away from the ideal I_h symmetry. A shift is also noticeable, corresponding to a charge transfer of ~ 2.7 e^-/C_{60}, affecting the whole matrix. The strong alteration of the SERS spectrum (band broadening, apparition of new frequencies) can be related, in the case of Ni, to significant cage distortions, due to orbital hybridization. In alloy films (Ni+Fe)/C_{60} [13] (x_{Ni}: 1 – 10 at%, x_{Fe}: 0.3 – 6 at%) SERS spectroscopy reveals dramatic distortions of cages by strong broadening of the Ag(2)

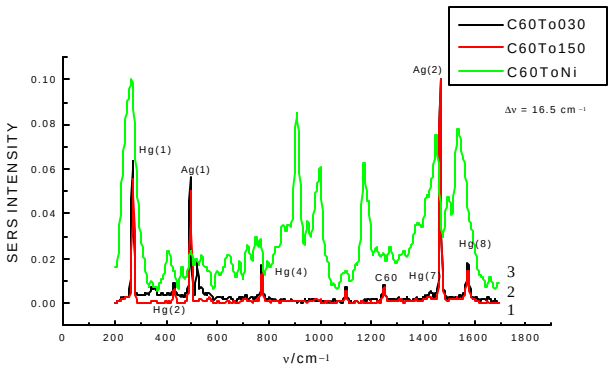

Fig. 2 SERS spectra for C_{60} films deposited at: 30ºC (2), 150ºC (1) and Ni/C_{60} film (15.9 at%, 3).

3.2 EXAFS EXPERIMENTS

EXAFS absorption spectroscopy at the CuK edge was used to investigate the local configuration around Cu atoms. Fig. 3 shows the Fourier transform of the EXAFS function, whose maxima stand for pair distances between the absorbing atom and first neighbors.

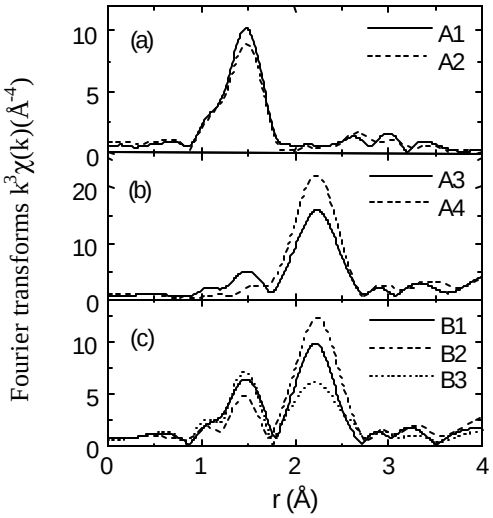

Fig. 3 Fourier transforms of Cu-K EXAFS in Cu-C_{60} thin films with Cu predominantly interstitial (a) or aggregated into metallic clusters (b,c).

Besides Cu–Cu bonds (at ~2.2 Å), originating in the cluster volume, Cu–C pairs (at ~1.5 Å), are present, at distances close to the sum of Cu^+ and C (covalent) radii. This observation suggests that interstitial Cu^+ might occupy tetrahedral and octahedral interstices in the fcc fullerite lattice. Another possibility (surface atoms in clusters) was also considered. The fraction X_{TEM} of surface

Cu was estimated using the average cluster radius from electron microscopy data [13]. On the other hand, another value X_{EX} can be derived from the area ratio of the EXAFS peaks. In cases where $X_{TEM} \approx X_{EX}$, surface Cu atoms are responsible for the Cu – C pairs. However, at low deposition rates of Cu – C_{60} films, $X_{EX} >> X_{TEM}$, pointing to a high fraction of interstitial ions (samples A1, A2, Fig.3a). The Cu diffraction patterns (Fig. 4) show a range of aspects. It can be seen that, when all Cu is interstitial (Fig. 3a) no diffraction lines are visible. On the contrary, when most of Cu is contained in clusters diffraction lines are present, supporting the assignment of the Fourier peaks in Fig. 3.

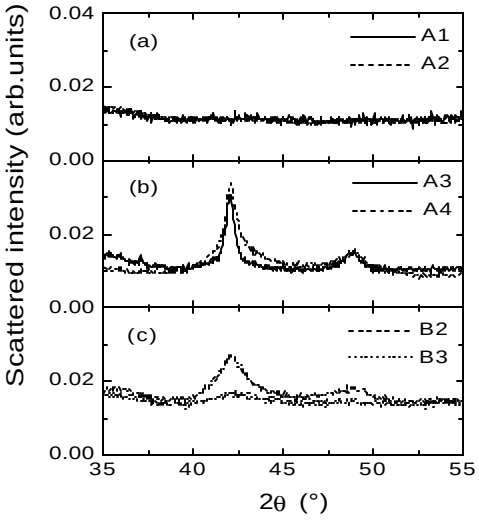

Fig. 4 Cu(111) and Cu(200) diffraction maxima (λ = 1.5 Å) of the Cu-C_{60} thin films.

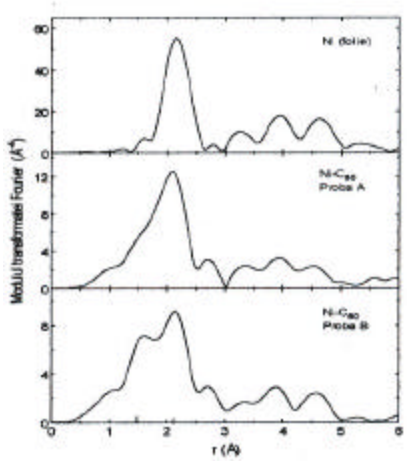

Fig.5 Module of the Fourier transform for a Ni foil and two (Ni+Fe)/C_{60} samples (B: 1.5 at% Ni, ~ 0.3 at% Fe, A: ~0.8 at% Ni)

EXAFS experiments at the NiK edge revealed a similar situation (Fig. 5) in (Ni+Fe)/C_{60} films [13]. Besides Ni-Ni pairs at ~2 Å (non-corrected value), an additional shoulder at 1.5 –1.6 Å should be assigned to Ni-C pair distances, mainly originating in interstitial Ni atoms.

These Ni atoms (or ions) could also exert a distorting influence on the C_{60} matrix, via electrostatic effects.

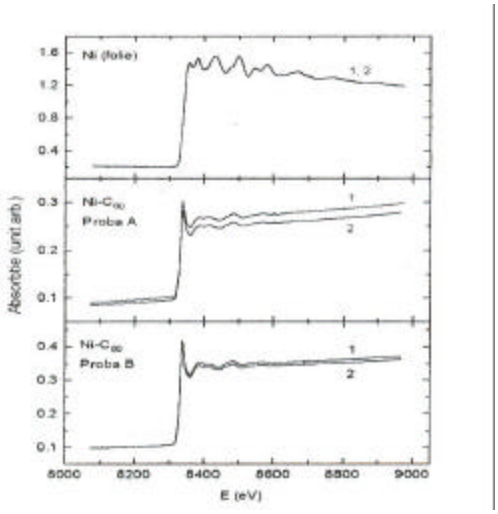

Fig. 6 Absorption jump at the NiK edge. Samples as in Fig. 5. Data of two runs are shown

Another observation concerns the strong increase of the "white line" in (Ni+Fe)/C_{60} films as compared to the Ni standard (Fig. 6). As the "white line" is due to transitions from $Ni1s_{1/2}$ levels to free p states above the Fermi level, this observation points to strong hybridization effects at the Ni-C_{60} interface. This hybridization should involve cluster surface atoms, but also interstitial ones.

3.3 EVALUATION OF CLUSTER STABILITY

Interstitial metal can be thought to originate in the energetical instability of statistically formed small clusters, which tend to decompose. Therefore, an evaluation of the average energy per atom E_a could help explain the experimental observations. E_a was calculated [8, 9] in a simple rigid band model, as $E_a = E_{coh} + E_S + E_{coul} + E_{dl}$, where the terms stand for the cohesive, surface (broken bonds), Coulomb and electric double layer (at cluster surface) energies. Clusters were considered as fully ionized by charge transfer. The resulting E_a, as a function of cluster radius R, was compared to E_a^0, calculated without the interface interaction terms (E_{coul}, E_{dl}) (Fig. 7). Thus, the effect of interface charge transfer on

cluster stability could be estimated. A critical cluster radius R_{cr} emerges (fig. 7). Clusters with $R<R_{cr}$ decompose down to interstitial ions while those with $R>R_C$ tend to grow, to decrease specific energy (in both cases). Beyond a radius R_0 clusters become stable ($E_a<0$).

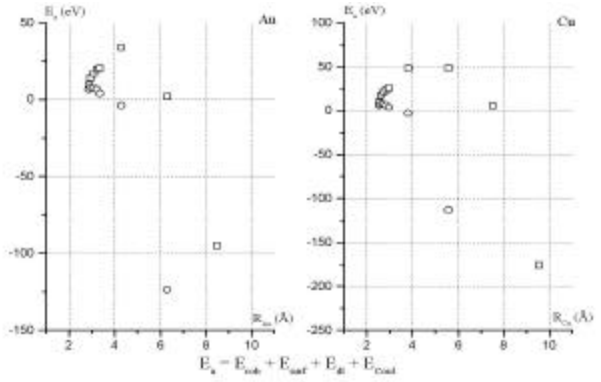

Fig. 7 Total energy per atom of metal clusters vs. radius R. : with interface charge transfer (E_a), o : without charge transfer (E_a^o).

Detailed calculations [8] showed that R_{cr} increases with increasing charge transfer Q. In a rigid-band model, Q takes the values 1.337 e^-/C_{60} for Cu and 1.019 e^-/C_{60} for Ni. Thus, charge transfer is more important in Cu/C_{60} systems than for Ni/C_{60}, in agreement with other experimental evidence. Correspondingly, critical radii R_{cr} are predicted as 4.8 and 3.8 Å for Cu and Ni, respectively. A higher R_{cr} could suggest that a broader range of small clusters will decompose to interstitials, i.e. that the interstitial fraction is higher.

The estimated R_0 value should be compared with the radius R_m of the smallest clusters observed by TEM. In the case of Cu/C_{60}, $R_m \approx 10$ Å [9], while $R_m \approx 9$ Å for Ni/C_{60} [11]. These values are close to the calculated R_0 of 8 Å(Cu) and 5 Å (Ni).

3.4 LATTICE DISTORTIONS IN FULLERITE

The presence of interstitial ions is expected to cause extensive lattice distortions in the C_{60} fullerite. This aspect was investigated by XRD [9], using both sealed – source and synchrotron radiation. The microstrain was estimated by the width Δk of the main (220) and (311) fullerite lines. As can be seen in Fig. 8, relatively strong distortions are noticed in the Cu – C_{60} films. They can be related to the high fraction of interstitial ions in the latter system.

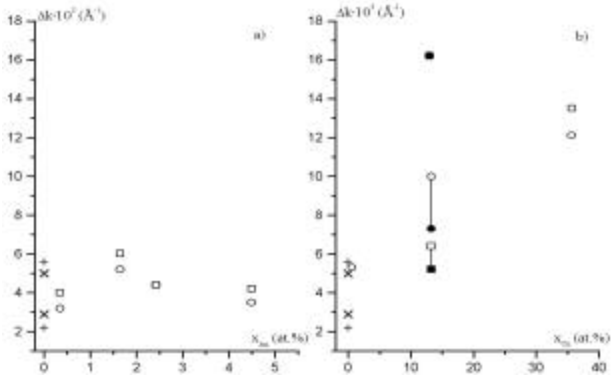

Fig. 8 FWHM data Δk for (220) (•, o) and (311) (■,) fullerite lines in Cu/C_{60} films. Empty symbols: sealed source. Full symbols: synchrotron source data. (+, x) (220) and (311) lines in two pure C_{60} films. Data belonging to the same sample are connected by vertical bars. $k = 2(\sin\theta)/\lambda$

An interesting aspect is the presence of microstrain in the metal clusters themselves. In Cu/C_{60} films, the metal clusters are well structured. The Ni/C_{60} samples show a quite different type of influence on the fullerite matrix (Fig. 9). Besides a fraction of crystalline C_{60}, an amorphous component appears in most samples, occasionally dominating the diffraction pattern (Fig. 9b). This amorphous modification of C_{60} is characterized by two broad peaks, *a* (k: 1.57+1.59 $Å^{-1}$) and *b* (k: 1.08-1.9 $Å^{-1}$, $k=2\sin\theta/\lambda$). Using a simple $\sin(kR)/kR$ approximation, R_a results as 12.2±0.1 Å, while R_b=8.4 Å. A first approximation model of this amorphous C_{60} could assign R_a to increased inter-cages distances, in fragments of disordered (111) planes (intercage distance: 10.04 Å). On the other hand, R_b could be contributed by random assemblies of distorted cages, with an average diameter R_b (instead of the correct 7.10 Å). The random packing of the cages could be favored by the strong distortions, evidenced by Raman spectroscopy.

3.5 MICROSTRUCTURE

Metal clusters in M – C_{60} films were visualized by transmission electron microscopy on thin sections (XTEM). Cluster sizes of 20 – 130 Å were noticed in Cu – C_{60} films (x_{Cu}: 0.6-36 at%) and 2-5 Å in Ni/C_{60} (x_{Ni}: 10-21 at%). HREM images reveal crystalline Cu clusters, where the (111) planes are visible.

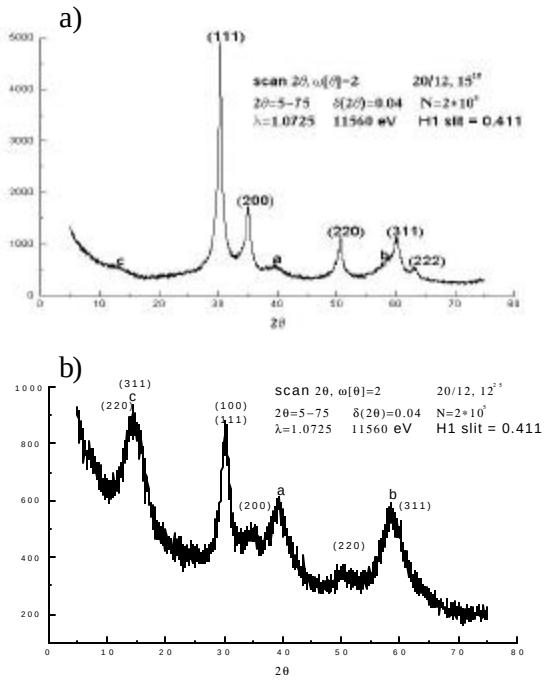

Fig. 9 Ni/C_{60} diffraction patterns. a: sample A4, b: sample A3

3.6 VALENCE ELECTRON STATES IN Cu CLUSTERS

X–ray emission spectroscopy of the CuL_α line yields important information on the distribution of occupied electronic states in Cu 3d bands.

The L_α line originates in transitions from (mainly) 3d states into the inner $2p_{3/2}$ level. For Cu clusters in Cu – C_{60} films a narrower line was noticed, also shifted to lower energies (Fig. 10), in comparison with bulk Cu.

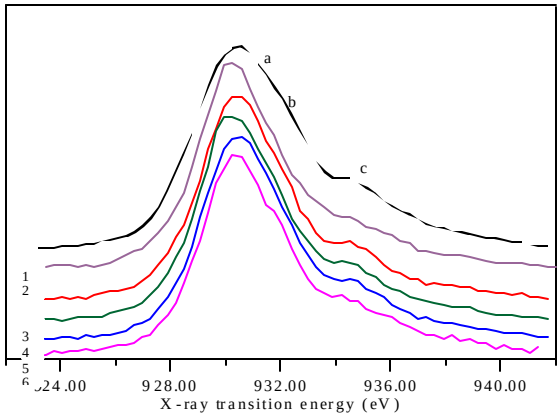

Fig. 10 CuL_α emission line in bulk (1) and in Cu/C_{60} samples. a, b, c: satellites. From top to bottom: Cu concentrations: 13, 13, 9, 21, 36 at%

These effects can be accounted for mainly by cluster size, the incomplete coordination in small clusters accounting for the narrowing of the valence band. However, a partial depletion of the 3d band due to charge transfer towards C_{60} could also play a role.

3.7 ELECTRICAL TRANSPORT

Doping C_{60} with metal is expected to introduce localized levels in the fullerite energy gap. Responsible for this should be, in the first line, the interstitial atoms and ions. In Cu – C_{60} films, metal doping was seen [15] to considerably increase the electrical conductivity σ, by charge transfer into the LUMO (conduction) C_{60} band.

Also, low–temperature $\sigma(T)$ behavior suggests hopping charge transport in a band of localized levels, at ~ 0.3 eV from the LUMO (conduction) band of C_{60}.

4. CONCLUSIONS

Metal – C_{60} thin-film nanosystems offer an optimal means of investigating interface interaction between metal and fullerite. A series of physical methods was applied to investigate the structure and physical properties of Cu – C_{60} and Ni– C_{60} films, with focus on the alterations of the C_{60} matrix. While charge transfer was seen to dominate at Cu/C_{60} interface, Ni behaviour was different. Evidence was brought forward for hybrid $C(\pi,\pi^*)$-Ni(s,d) bond formation at interfaces, causing strong distortions of the C_{60} cages. A model was derived, concerning metal cluster behavior in a C_{60} matrix. Charge transfer at interface results as the main interaction process, especially in Cu – based systems.

ACKNOWLEDGEMENTS

We are highly indebted to the Alexander Von Humboldt Foundation for financial support. The work was partially supported by CNCSIS Grant 80/1237.

REFERENCES

1. A. J. MAXWELL, P.A. BRÜHWILER, D. ARVANITIS et al: Phys. Rev. B Vol. 57 (1998) 7312
2. S. MODESTI, S. CERASARI, P. RUDOLF: Phys. Rev. Lett. Vol. 71 (1993) 2469
3. R. MANAILA, A. BELU – MARIAN, D. MACOVEI et al: J. Raman Spectrosc. Vol. 30 (1999) 1019
4. S.J. CHASE, W.S. BACSA, M.G. MITCH et al: Phys. Rev. B Vol. 46 (1992) 7873
5. M. PEDIO, K. HEVESI, N. ZEMA et al: Surf. Sci. Vol. 437 (1999) 249
6. K.-D. TSUEI, J.-Y. YUH, C.-T.TZENG et al: Phys. Rev. B Vol. 56 (1997) 15412
7. K.-D. TSUEI, P.D. JOHNSON: Solid State Commun. Vol. 101 (1997) 337
8. R. POPESCU, D. MACOVEI, R. MANAILA et al: Mater. Sci. Forum Vol. 321 – 324 (2000) 554
9. R. POPESCU, D. MACOVEI, A. DEVENYI et al: Eur. Phys. J. B Vol. 13 (2000) 737
10. A. DEVENYI, A. BELU – MARIAN, R. MANAILA et al: Proc. EUROMAT 99 Vol. 10 (2000)
11. S. POENARIU, C TEODORESCU, D. MACOVEI, J.L. Labar, A. Devenyi, R. Manaila (to be published)
12. M.G. MITCH, J.S. LANNIN: Phys. Rev. B Vol. 51 (1995) 6784
13. S. POENARIU, A. DEVENYI, TH. MARIAN, R. MANAILA (in preparation)
14. E. BELIN – FERRE, R. POPESCU, R. MANAILA et al: to be published
15. A. BELU – MARIAN et al: unpublished results

Received June 6, 2002